Journal of Materials Chemistry A

Accepted Manuscript

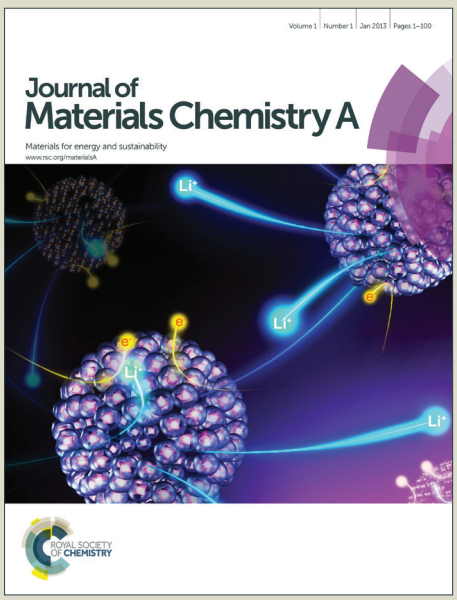

ROYAL SOCIETY OF CHEMISTRY

www.rsc.org/materialsA

Journal Name

Dynamic Article Links ►

Cite this: DOI: 10.1039/c0xx00000x

www.rsc.org/xxxxxx

ARTICLE TYPE

A two-dimensionally microporous thiostannate with superior Cs^+ and Sr^{2+} ion-exchange property

Xing-Hui Qi[a, b], Ke-Zhao Du[a], Mei-Ling Feng*[a], Jian-Rong Li[a], Cheng-Feng Du[a, c], Bo Zhang[a, c] and Xiao-Ying Huang[a]

Received (in XXX, XXX) Xth XXXXXXXXX 20XX, Accepted Xth XXXXXXXXX 20XX
DOI: 10.1039/b000000x

The removal of highly-radioactive and long-lived $^{137}Cs^+$ and $^{90}Sr^{2+}$ from solution is of significance for radionuclide remediation. Herein we prepared a two-dimensionally microporous thiostannate, namely $(Me_2NH_2)_{4/3}(Me_3NH)_{2/3}Sn_3S_7 \cdot 1.25H_2O$ (FJSM-SnS), and systematically investigated its Cs^+ and Sr^{2+} ion-exchange performance in different conditions. The structural stabilities and variation, ion-exchange kinetic and isothermal studies, pH dependent distribution coefficients (K_d), ion-exchange in the simulated groundwater and ion-exchange applied chromatography have been investigated. The results indicated that the maximum Cs^+ and Sr^{2+} ion-exchange capacities of FJSM-SnS were 408.91 mg/g and 65.19 mg/g, respectively. In particular, the FJSM-SnS showed quick ion-exchange ability and wide pH resistance (0.7 ~ 12.7) which make it outstanding among the ion-exchangers. The ion-exchange chromatographic column was firstly studied for chalcogenido ion-exchange materials, that is, a column filled with 3.0 g FJSM-SnS could remove 96% ~ 99% of Cs^+ ion and near 100% of Sr^{2+} ion at low ionic concentrations in 900 bed volumes solutions, respectively. Furthermore, the title material could be synthesized in large-scale by a facile, one-pot and economically solvothermal method. The relatively low-cost but remarkable ion-exchange performance makes it promising for radionuclide remediation.

Cite this: DOI: 10.1039/c0xx00000x

www.rsc.org/xxxxxx

ARTICLE TYPE

1. Introduction

Today, with the nuclear energy development, the problem of radioactive wastes has become more and more thorny. The removal of toxic radioactive contaminants for further treatment and disposal is of vital significance. For example, there are dilute radioactive ions with thick additional ions in the nuclear waste.[1-4] Among them, $^{137}Cs^{+}$ and $^{90}Sr^{2+}$ ions are the most hazardous and long-lived byproducts with high concentration of Na^{+} (> 5 mol/L).[5-10] Thus far, a number of methods have been developed to treat the aqueous radioactive wastes including ion-exchange, precipitation, evaporation, reverse osmoses, ultrafiltration, microfiltration and solvent extraction.[11] The ion-exchange treatment is attractive for the high selectivity, minimum solidified waste and reductive radioactive discharge.[12, 13] The ion-exchangers could be divided into the inorganic and organic materials.[14, 15] Considering that in the highly-radioactive solution the organic ion-exchangers could be damaged by hydrolysis of functional groups, chain scission and changes in degree of crosslinking, the inorganic ion-exchanger is screened out for the superior chemical, thermal, radiation resistance, and easily immobilizing for use and then disposing off after use.[16, 17] The typical inorganic ion-exchangers such as the natural minerals (zeolites and clays),[18-22] insoluble transition metal ferrocyanides,[23, 24] and titanium silicates have been studied.[25-28] However, the natural minerals and silicates would be ineffective at extreme pH for the dissolution of aluminate and protons inhibiting effect. While the microcrystalline nature of ferrocyanides renders their application in column mode operations.[23] In recent years, the open-framework metal chalcogenides as ion-exchangers have caught increasing attention owing to their high ion-exchange capacity and high selectivity.[29-36] The advantages of chalcogenido ion-exchangers originate from their more flexible frameworks compared to those of oxide ion-exchangers and the favorable interactions between the soft Lewis basic Q^{2-} (Q = S and Se) ions and the soft Lewis acidic metal ions.[37, 38] .

Some inorganic crystalline chalcogenido ion-exchangers have been reported, such as KBi_3S_5,[39, 40] $K_{14}Cd_{15}Sn_{12}Se_{46}$,[41] $K_6Sn[Zn_4Sn_4S_{17}]$,[35, 36] $(NH_4)_4In_{12}Se_{20}$,[37] $K_{2x}Mn_xSn_{3-x}S_6$ (KMS-1)[33, 34, 42] and $K_{2x}Mg_xSn_{3-x}S_6$ (KMS-2),[3] in which the K^{+} and NH_4^{+} are able to be exchanged by the Cs^{+}, Sr^{2+} and some other heavy metal ions. Recently, much considerable progress has been made in the search of chalcogenido ion-exchange materials with the organic amine cations as counterions and structural directing agents (SDAs), as the organic amines feature large size tunability and conformational flexibility. Significant examples include $[(CH_3CH_2CH_2)_2NH_2]_5In_5Sb_6S_{19}\cdot1.45H_2O$,[38] $[(Me)_2NH_2]_2Ga_2Sb_2S_7\cdot H_2O$,[32] $[(Me)_2NH_2]_2[GeSb_2S_6]$[43] and $[(Me)_2NH_2]_{0.75}[Ag_{1.25}SnSe_3]$.[44] Nevertheless, the research on crystalline chalcogenido ion-exchangers is still in a fledging period. In particular, the development of new superior chalcogenido ion-exchangers, which are structurally robust and uniform, easily synthesized and highly cost-efficient, remains a challenge towards practical applications. Hitherto, several worthy compounds are limited to KMS-1 ($K_{2x}Mn_xSn_{3-x}S_6$),[30, 33, 34, 45, 46] LHMS ($H_{2x}Mn_xSn_{3-x}S_6$)[47] and KMS-2 ($K_{2x}Mg_xSn_{3-x}S_6$).[3] But they are all restricted to the Mn/Mg-Sn-S frameworks. The valence of manganese in KMS-1 and LHMS is unstable and the indefinite element proportion may impact the uniformity of the product in magnifying synthesis. Comparatively speaking, the thiostannates are relatively inexpensive and usually present stable and uniform open frameworks. For example, layered $A_2Sn_3S_7$ (A = cations) are easily synthesized with very robust and flexible frameworks, but their Cs^{+} and Sr^{2+} ion-exchange properties haven't been reported.

Herein we designed a new thiostannate as superior ion-exchange material, namely $[Me_2NH_2]_{4/3}[Me_3NH]_{2/3}Sn_3S_7\cdot1.25H_2O$ (denoted as FJSM-SnS). It could be easily synthesized in large-scale by a facile, one-pot and economically solvothermal method. The structural characterizations and ion-exchange properties of FJSM-SnS have been studied thoroughly. The results indicated that the ion-exchanges for Cs^{+} and Sr^{2+} could reach rapid equilibrium within 5 minutes, which is much faster than those of most of the ion-exchangers.[48] The Cs^{+} and Sr^{2+} equilibrium isotherms fit the Langmuir model well with the maximum Cs^{+} and Sr^{2+} exchange capacities of 408.91 mg/g and 65.19 mg/g, respectively. More importantly, the material could keep its robust framework and effective distribution coefficient over wide pH range (0.7 ~ 12.7) and various simulated environments during the ion-exchange processes. Furthermore, the simple ion-exchange chromatographic column filled with 3.0 g FJSM-SnS could remove 96% ~ 99% Cs^{+} and near 100% Sr^{2+}, respectively, at low ion concentrations in 900 bed volumes solutions.

2. Experimental section

2.1 Material Synthesis

All reagents and chemicals were purchased from commercial sources without further purification. Synthesis of $(Me_2NH_2)_{4/3}(Me_3NH)_{2/3}(Sn_3S_7)\cdot1.25H_2O$: A mixture of $SnCl_4\cdot5H_2O$ (1.4 mmol, 0.502 g), S (4 mmol, 0.131 g) in 3 mL dimethylamine (38% ~ 41%) and 1 mL water was stirred under ambient conditions until homogeneous. The resulting mixture was sealed in a 20 mL stainless steel reactor with a Teflon liner, heated at 180 °C for 7 days and then cooled to room temperature. Yellow hexagonal crystals of the title compound and tiny indefinite yellow powders were obtained by filtration. The crystalline products were washed by ethanol, and air-dried (Yield: 0.270 g, 80.35% based on Sn). Anal. calc. for $N_{24}C_{56}H_{238}Sn_{36}S_{84}O_{15}$: C, 7.96%; H, 2.84%; N, 3.98%. Found: C, 8.05%; H, 2.78%; N, 4.06%. Large scale synthesis of $(Me_2NH_2)_{4/3}(Me_3NH)_{2/3}(Sn_3S_7)\cdot1.25H_2O$: a mixture of $SnCl_4\cdot5H_2O$ (11.5 mmol, 4.047 g), S (28 mmol, 0.896 g) in 24 mL dimethylamine (38% ~ 41%) and 8 mL water was stirred

under ambient conditions until homogeneous. The resulting mixture was sealed in a 235 mL stainless steel reactor with a Teflon liner, heated at 180 °C for 7 days and then cooled to room temperature. Yellow hexagonal crystals of the title compound and tiny indefinite yellow powders were obtained by filtration. The crystalline products were washed by ethanol and air-dried (Yield: 2.062 g, 76.3% based on Sn).

2.2 Physical Measurements

Elemental analyses of C, H, and N were carried out on a German Elementary Vario EL III instrument. Energy-dispersive spectroscopy (EDS) and SEM analyses were performed with a JEOL JSM-6700F scanning electron microscope and HITACHI FE-SEM SU8010. The transmission electron microscope (TEM) was performed on FEI Tecani G2 F20. FT-IR spectra (KBr pellet) were recorded on a Magna 750 FTIR spectrometer in the range of 4000-400 cm^{-1}. The UV/Vis spectra were measured by using $BaSO_4$ as a standard (100% reflectance) at room temperature with a Perkin-Elmer Lambda 900. Powder X-ray diffraction (PXRD) patterns were obtained from a Miniflex II diffractometer at 30 kV and 15 mA using Cu$K\alpha$ (1.54178 Å) in the angular range of 2θ = 3-65° at room temperature. The simulated PXRD pattern through single crystal data was generated by using the PowderCell program. The thermogravimetric (TG) analyses were performed on a NETZSCH STA449C thermogravimetric analyzer with a heating rate of 5 °C/min under a nitrogen atmosphere and the TG-MS was carried on a STA449C-QMS403C. The Inductively Coupled Plasma (ICP) analyses were performed on an Ultima 2 unit. The Atomic Absorption Spectroscopy (AAS) were carried on a ContrAA 700. The Single-crystal X-ray diffraction data for FJSM-SnS were collected on a SuperNova CCD diffractometer with graphite-monochromated Mo$K\alpha$ (0.71073 Å) at 100(2) K. The single-crystal X-ray diffraction data for FJSM-SnS-Cs were collected on an Oxford Xcalibur Eos CCD diffractometer with graphite-monochromated Mo$K\alpha$ (0.71073 Å) at room temperature. The structures were solved by direct methods and refined by full-matrix least-squares on F^2 by using the program SHELX-97. An empirical absorption correction was applied using the multi-scan method; CCDC 1025383 for FJSM-SnS and CCDC 1025384 for Cs^+-exchanged FJSM-SnS.

2.3 Ion-exchange Experiments

A typical ion-exchange experiment of FJSM-SnS with ACl (A = Cs^+, Sr^{2+}) is as follows. In a solution of ACl, the ground polycrystalline powders of FJSM-SnS were added. The mixture was kept under magnetic stirring for ~ 20 min at 65 °C. Then the yellow polycrystalline materials were separated by centrifugation and washed several times with deionized water. The concentrations of Cs^+ and Sr^{2+} in the clear supernatant were determined by Inductively Coupled Plasma (ICP) or Atomic Absorption Spectroscopy (AAS).

Kinetic and isotherm experiments: In kinetic experiments, the solutions of Cs^+ (128 ppm) and Sr^{2+} (44.31 ppm) were prepared individually at neutral condition. *V:m* is 278 mL/g for Cs^+ (*V* = 5 mL, *m* = 18 mg) and *V:m* is 1000 mL/g for Sr^{2+} (*V* = 10 mL, *m* = 10 mg), respectively. All the samples were put in the 65 °C water bath under magnetic stirring. Then we took one sample one time at different time of ion-exchange. In isotherm experiment, the solutions of Cs^+ and Sr^{2+} with different concentrations were prepared, respectively. The *V:m* of all the samples is 1000 mL/g (*V* = 18 mL, *m* = 18 mg). The ion-exchange lasted about 20 min. Then all the samples were taken out and processed.

The pH dependent experiments: The solutions of Cs^+ and Sr^{2+} with different pH were prepared. The initial concentrations are around 5 ~ 7 ppm for Cs^+ ion and 2 ~ 7 ppm for Sr^{2+} ion, respectively. And *V:m* is 1000 mL/g (*V* = 18 mL, *m* = 18mg). The pH was regulated by NaOH or HCl. Then the typical ion-exchange experiments were carried on. The competitive ion-exchange experiments with the coexistence of Cs^+ and Sr^{2+} ions in different pH were performed in a similar way.

In the simulated groundwater: The aqueous solution with ~ 8 ppm Ca^{2+}, 77 ppm Na^+, 8 ppm Mg^{2+}, 6 ppm K^+ and 2 ppm Cs^+ ions was used to simulate Cs^+-contaminated neutral groundwater and the aqueous solution with ~ 7 ppm Ca^{2+}, 232.5 ppm Na^+, 9.7 ppm Mg^{2+}, 9.1 ppm K^+ and 6 ppm Sr^{2+} to simulate Sr^{2+}-contaminated neutral groundwater, respectively. Such solutions with adjusted pH of ~11 were used to simulate typical alkaline groundwater contaminated with Cs^+ and Sr^{2+} ions, respectively. The initial concentrations of Cs^+ and Sr^{2+} were about 2 ppm and 6 ppm with the *V:m* = 1000 mL/g, respectively.

Ion-exchange chromatographic column: A column with inside diameter of 13.4 mm was filled with 3 g FJSM-SnS crystals. The height of the filler was about 10 cm with a sealed empty glass tube (outside diameter = 12 mm) in the centre of the column. Then a mixing solution of Cs^+ and Sr^{2+} flowed through the ion-exchange chromatographic column at room temperature. The initial Cs^+ concentration is in the range of 12 ~ 14.5 ppm and initial Sr^{2+} concentration is 5.98 ~ 8.2 ppm. AAS and ICP were used to track the Cs^+ and Sr^{2+} concentrations in the outlet solution.

3. Results and discussion

3.1 Structural characterizations

The yellow hexagonal crystals are stable in air (Fig. 1a). Before the ion-exchange experiments, the phase purity was confirmed by PXRD on the selected polycrystalline sample, Fig. 1b. Various analytic techniques were employed to confirm that the formula of FJSM-SnS was $(Me_2NH_2)_{4/3}(Me_3NH)_{2/3}Sn_3S_7\cdot 1.25H_2O$. Especially, the TG-MS analyses were used to track the components of $[Me_2NH_2]^+$ and $[Me_3NH]^+$ (Fig. S1). The TG-MS results showed that at the weight-loss step around 200 °C, the characteristic mass peaks of $[Me_3NH]^+$, $[Me_2NH_2]^+$ and H_2O could be detected. So the weight-loss was mostly attributed to the removal of Me_3N, Me_2NH, H_2O and one H_2S molecule per formula (theoretical weight loss: 22.17%, found: 22.21%) before 200 °C. It is noted that the Me_3N hasn't been used in the synthesis. To find out the origin of $[Me_3NH]^+$ ion, the mass spectra of the Me_2NH aqueous solution and that of the solution after solvothermal reaction have been compared. It is clear that the proportion of the $[Me_3NH]^+$ dramatically increased after the reaction (Fig. S2). Based on the results of the mass spectra, the unexpected $[Me_3NH]^+$ should be in-situ generated from the solvent Me_2NH.[49]

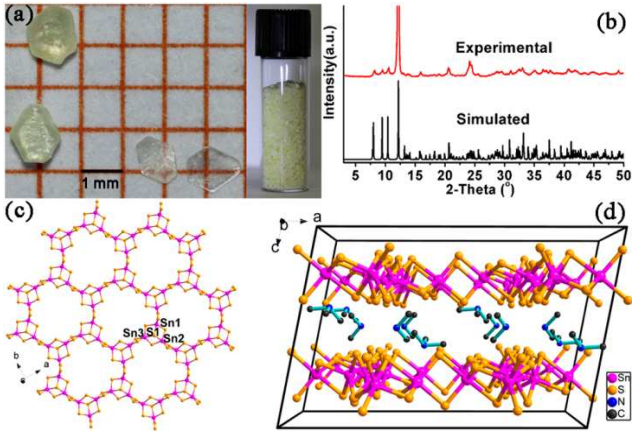

Fig. 1 (a) Photographs of FJSM-SnS crystals; (b) experimental and simulated PXRD patterns of FJSM-SnS; (c) a 2D $[Sn_3S_7]_n^{2n-}$ anionic layer parallel to the *ab* plane; (d) packing of the layers in FJSM-SnS in a perspective view along the *b*-axis. The H_2O molecules and H atoms of organic amines are omitted for clarity.

Single crystal X-ray crystallography reveals that FJSM-SnS belongs to the space group *C*2/*c* with cell parameters of a = 22.5651(10), b = 13.0672(6), c = 14.8064(13) Å and β = 101.227(6)°, V = 4282.3(5) Å^3, Z = 8. The compound features a microporous layered structure, similar to those of the tin sulfides Cs-SnS-1,[50] TMA-SnS-1a,[51] and DABCOH-SnS-1.[52-54] All the Sn atoms are five-coordinated with S to form SnS_5 trigonal bipyramids. Three SnS_5 trigonal bipyramids are fused into a $[Sn_3S_{10}]$ unit with a $[Sn_3S_4]$ semi-cubane-like core by edge-sharing. Then each $[Sn_3S_{10}]$ unit connects to other three such units by edge-sharing, resulting in a 2D $[Sn_3S_7]_n^{2n-}$ anionic layer parallel to the *ab* plane, in which there exist windows formed by twenty-four-membered $[Sn_{12}S_{12}]$ rings from six $[Sn_3S_4]$ cores (Fig. 1c). The 2D $[Sn_3S_7]_n^{2n-}$ layers are stacked in *AA* sequence along the *c*-axis (Fig. 1d). The interlayer distance is estimated to be 7.258 Å.[30] The $[Me_2NH_2]^+$, $[Me_3NH]^+$ cations and lattice water molecules are located at the interlayer spaces.

Since the pioneer work by Ozin et al., $A_2Sn_3S_7$ has received much attention for its unique robust and flexible framework that can undergo elastic deformations in response to a variety of cations.[52-59] The voids within and between the layers could be adjusted by different templating cations, for example, $[Me_4N]^+$,[59] Rb^+,[60] Cs^+,[50] $[Me_3N]^+$,[51] $[DABCOH]^+$ (protonated 1,8-diazabicyclooctane),[52] QUIN (QUIN = quinuclidinium),[55] TBA (TBA = tert-butylamine),[55] $[NH_4]^+$ and $[Et_4N]^+$ ($[Et_4N]^+$ = tetraethylamine).[54] The performances of $A_2Sn_3S_7$, such as gas adsorption and discrimination, chemical sensing and amine exchange, have been studied in the previous works. In the case of ion-exchange property, there was only one example demonstrating partial $[Me_4N]^+$ exchange with the Na^+, Ca^{2+}, Co^{2+} and Ni^{2+} ions in $[Me_4N]_2Sn_3S_7{\cdot}H_2O$.[59] Up to now, the applications of this series of compounds in Cs^+ and Sr^{2+} ion-exchanges have not been mentioned.

3.2 The variation of structure and optical properties

The structural stability of FJSM-SnS in the Cs^+ and Sr^{2+} solutions has been considered before the subsequent systematic ion-exchange investigations. Scanning electronic microscope (SEM) analyses indicated that FJSM-SnS could still maintain the crystal shape after ion-exchange. The layered nature was more distinct after the inorganic ions intercalated into the layers, Fig. 2a-c. The PXRD patterns of the Cs^+ and Sr^{2+}-exchanged materials retained similar to that of the pristine (Fig. 2d). The results of SEM and PXRD of ion-exchanged products indicated that the title compound with a robust framework was stable under humid atmosphere. The band gap of the pristine compound is about 2.92 eV, while it is 2.82 eV and 2.60 eV for the Cs^+- and Sr^{2+}-exchanged products, respectively (Fig. 2e). The narrower band gaps are consistent with the deeper colors of the Cs^+- and Sr^{2+}-exchanged materials. The shifts of the optical absorption edges should be attributed to the charge transfer between the sulfur ligands of inorganic layers and the inserted Cs^+ and Sr^{2+} ions. Similar phenomena have been also found in other Cs^+ and Sr^{2+} ion-exchange materials such as KMS-2.[3]

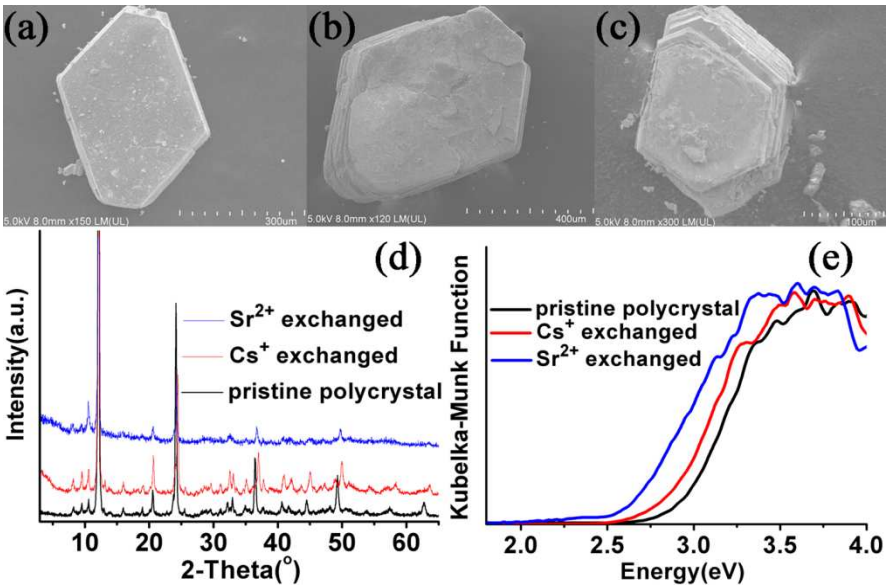

Fig. 2 SEM images of pristine FJSM-SnS crystals (a), the Cs^+-exchanged (b) and the Sr^{2+}-exchanged (c) ones, PXRD patterns (d) and solid-state optical absorption spectra (e) of the pristine FJSM-SnS, Cs^+ and Sr^{2+}-exchanged products.

Cite this: DOI: 10.1039/c0xx00000x

www.rsc.org/xxxxxx

ARTICLE TYPE

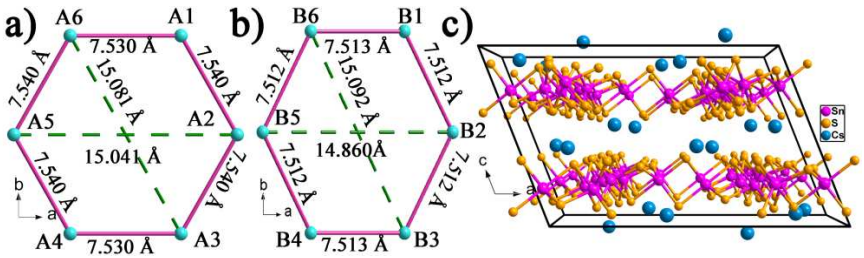

Fig. 3 The simplified hexagon with Sn_3S_4 as a node and (μ–S)$_2$ as a ligand in FJSM-SnS (a) and FJSM-SnS-Cs (b); packing of FJSM-SnS-Cs (c).

The single crystal X-ray crystallography data of Cs^+-exchanged FJSM-SnS has been collected ($Cs_2Sn_3S_7{\cdot}4.5H_2O$, denoted as FJSM-SnS-Cs) to further understand the ion-exchange mechanism. $Cs_2Sn_3S_7{\cdot}4.5H_2O$ (FJSM-SnS-Cs) is isostructural to the previously reported $Cs_2Sn_3S_7{\cdot}1/2S_8$ (Cs-SnS-1).[50] The formula has been confirmed by the TG-MS (Fig. S5) and EA results (Found, C/N = 0 and H = 1.00%; Calculated: C/N = 0 and H = 0.98%). It also belongs to the *C*2/*c* space group with cell parameters of a = 22.363(5), b = 13.0895(16), c = 14.432(3) Å and β = 111.60(2)°, V = 3927.6 (13) Å^3, Z = 8. Compared to those of the pristine, the c-axis constricts ~ 0.37 Å while the β expands from 101.227(6)° to 111.60(2)° in the FJSM-SnS-Cs unit cell. There is only a little distortion of the windows formed by the twenty-four-membered [$Sn_{12}S_{12}$] rings from six [Sn_3S_4] cores in the $[Sn_3S_7]_n^{2n-}$ layer. For a clearer comparison, a hexagonal window was brought out with [Sn_3S_4] as a node and (μ–S)$_2$ as a ligand, respectively. All the lengths of sides shrink 0.1 ~ 0.3 Å after Cs^+-exchange while the diagonal lengths of the hexagonal window mentioned above change from 15.04 × 15.08 × 15.08 Å to 14.86 × 15.09 × 15.09 Å (Fig. 3a and 3b). The interlayer distance condenses from 7.258 to 6.709 Å (Fig. 1d and 3c), which is in accordance with the shift towards the higher 2θ angles in the PXRD patterns after ion-exchange (Fig. 2d). The structural variation described above might spring from the strong affinity of Cs^+ to the soft basic framework. The flexible framework of FJSM-SnS, which has an intermediate character between the layered chalcogenide and porous molecular sieves, should play an important role in the extraordinary ion-exchange performance.

Besides the above mentioned characterizations, the ion-exchange properties for Cs^+ and Sr^{2+} ions were also confirmed by EDS (Fig. S6), ICP and AAS.

3.3 Kinetic and isotherm studies of ion exchange

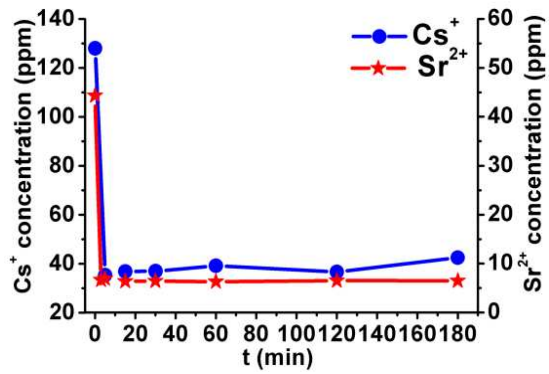

Fig. 4 Kinetics of Cs^+ and Sr^{2+} ion-exchange of FJSM-SnS plotted as the Cs^+ and Sr^{2+} ion concentration (ppm) *vs* the time t (min), respectively.

Table 1 The equilibrium time of different materials

Compound	Equilibrium time for Cs^+ (temperature)	Equilibrium time for Sr^{2+} (temperature)
FJISM-SnS (This report)	5 min (65 °C)	5 min (65 °C)
	30 min (17 °C)	60 min (17 °C)
KMS-1[33, 34]	5 min (UM[a])	> 2 h (UM)
KMS-2[3]	10~15 h (UM)	10~15 h (UM)
$K_6Sn[Zn_4Sn_4S_{17}]$[35]	> 12h (RT)	------
zeolite A[61]	90~120 min (20~60 °C)	90~120 min (20~60 °C)
Indium Sulphide[17]	------	60 min (UM)
UCR-28[62]	------	90~120 min (RT)
H-CST[25]	60 min (25 °C)	------
GaSbS[48]	15 h (UM, SW[b])	------
K-SGU-45[48]	15 h (UM, SW)	------
Na-CST[48]	15 h (UM, SW)	------
Na-PMica[48]	15 h (UM, SW)	------
CHA[48]	15 h (UM, SW)	------
ETS-10[63]	50 min (40 °C)	------
	50 min (20 °C)	
	> 160 h (4 °C)	
ETS-4[64, 65]	> 10 h (RT[c])	24 h (RT)
AM-2[66]	> 400 h (90 °C)	> 400 h (90 °C)
UOP IONSIV IE-911[67]	> 4 h (23 °C, 1 *M* Na^+ solution)	> 4 h (23 °C, 1 *M* Na^+ solution)

[a]UM = unmentioned; [b]SW = seawater; [c]RT = room temperature.

The kinetics and isotherms of Cs^+ and Sr^{2+} ion-exchanges have been studied. As shown in Fig. 4, the concentrations of Cs^+ (128 ppm) and Sr^{2+} (44.31 ppm) ions vertically decreased and reached their equilibriums within 5 minutes at 65 °C. The Cs^+ and Sr^{2+} ion-exchanges are much faster than those of most of the ion-exchangers including the vanadosilicate SGU-45 (noted as the most effective Cs^+ remover,[48] Table 1). This should be attributed to the flexible porous framework, the higher affinity of the chalcogenide for the soft Cs^+ and Sr^{2+} ions and the excellent ion-exchange abilities of small organic amines. There is an obvious fluctuation in the kinetic curve of Cs^+ ion-exchange compared to that of Sr^{2+} ion, which could be attributed to the dynamic Cs^+-exchange process.[33] The Cs^+ ion replaced the $[Me_2NH_2]^+$ or $[Me_3NH]^+$ cations immediately at the beginning and progressively a small fraction of $[Me_2NH_2]^+$ or $[Me_3NH]^+$ re-entered the interlayer spaces releasing some Cs^+ ion back to the solution. In contrast, the Sr^{2+}-exchange kinetic curve is almost flat according to the larger volume and higher affinity of Sr^{2+}, which make the dynamic process calmer. In addition, the kinetic studies at room temperature (RT) have been performed (Fig. S7). The results indicated that the compound still retained its abilities of fast ion-capture at RT. At RT, the ion-exchange equilibrium for Cs^+ ions could be reached within 30 minutes while that for Sr^{2+} ions was extended to 60 minutes (Table 1). The equilibrium time is longer time than that at 65 °C (5 minutes for Cs^+ and Sr^{2+}), but is still comparable to those of the other ion exchangers including the commercial UOP IONSIV IE-911 whose equilibrium time is more than 4h.[62-72]

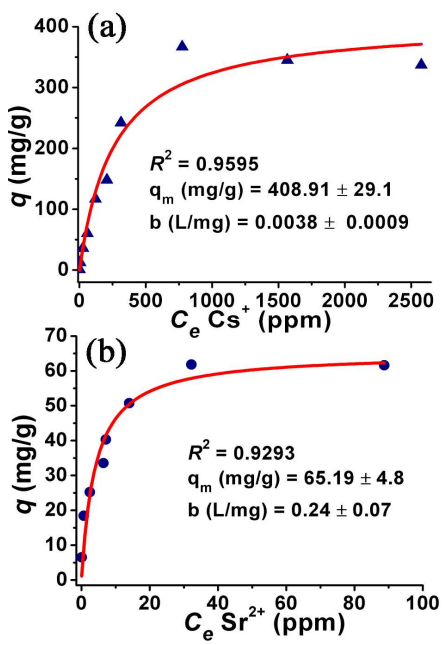

Fig. 5 Cs^+ (a) and Sr^{2+} (b) equilibrium curves for FJSM-SnS (pH ≈ 7, *V*:*m* = 1000 mL/g, contact time 20 min, at 65 °C, initial Cs^+ and Sr^{2+} concentrations in the range of 1-2920 ppm and 6-151 ppm, respectively). Langmuir equilibrium isotherms are derived from the Cs^+ and Sr^{2+} concentration at equilibrium plotted against the capacity (mg ions removed/g of ion-exchanger).

The Cs^+ equilibrium curve is graphed in Fig. 5a, which is derived from the Cs^+ concentration at equilibrium plotted against the capacity of Cs^+-exchange. Langmuir model could fit the equilibrium isotherm very well with the R^2 = 0.9595. The model is based on the assumptions that the surface containing the equivalent adsorbing sites is homogeneous, the state of the exchanged ions in the structure is definite, the ions on adjacent sites are independent and each site can catch only one ion.[61, 73] It can be described by the equation 1.

$$q = q_m \frac{bC_e}{1+bC_e} \qquad (1)$$

Where q (mg/g) is the amount of the ion exchanged at the equilibrium concentration C_e (ppm), q_m is the maximum exchange capacity of the exchanger, and b (L/mg) is the Langmuir constant related to the free energy of the exchange. The value of q can be calculated from the equation 2.

$$q = \frac{(C_0 - C_f)V}{m} \qquad (2)$$

Where C_0 and C_f (ppm) are the initial and equilibrium concentrations, respectively, which could be determined by the AAS or ICP method. V (mL) is the volume of the solution and m (g) is the amount of the ion-exchanger used in the experiment.

From the Fig. 5a, the maximum Cs^+ exchange capacity q_m of FJSM-SnS is 408.91 ± 29.1 mg/g, close to its theoretical ion-exchange capacity (377.2 mg/g). It is worth noting that the q_m of FJSM-SnS for Cs^+ ion is 1.8 times of that of KMS-1 (226 mg/g) and far more than those of commercial AMP-PAN (81 mg/g) and TAM-5 (191.8 mg/g) which are currently marketed by UOP as IONSIV IE-910 and IE-911.[33, 67, 70-72]

The Sr^{2+} equilibrium curve is graphed in Fig. 5b, which is derived from the Sr^{2+} concentration at equilibrium plotted against the capacity of Sr^{2+}-exchange. The Sr^{2+} equilibrium isotherm also fits the Langmuir model at the R^2 = 0.9293. The maximum Sr^{2+} exchange capacity q_m of FJSM-SnS is 65.19 ± 4.8 mg/g, which is about 4 times of that of the commercial AMP-PAN (15 mg/g).[70] The q_m of FJSM-SnS for Sr^{2+} ion is about 52% of the theoretical ion-exchange capacity (124.32 mg/g). This is probably attributed to the large volume of $[Sr(H_2O)_6]^{2+}$ as Sr^{2+} enters the structure in a hydrated form, while the interlayer space of FJSM-SnS is too small to load the full stoichiometric number of such large ions. Thus the Sr^{2+}-exchanged product still contained organic counter ions, which has been confirmed by the elemental analyses of C, H, and N (C, 3.92%; H, 2.84%; N, 1.55%). The similar phenomena have also been found in the layered metal sulfide KMS-1 and KMS-2.[3, 34]

3.4 pH dependent ion exchange experiments

Following the kinetic and isotherm studies, the pH dependent experiments of FJSM-SnS have been conducted. The distribution coefficient K_d was measured at various pH conditions. As a measurement of affinity and selectivity, K_d is described as follows:

$$K_d = \frac{V}{m}\frac{(C_0 - C_f)}{C_f} \qquad (3)$$

In equation 3, C_0 and C_f represent the initial and equilibrium ions concentration, V is the volume (mL) of the testing solution and m is the mass of the ion exchanger (g).

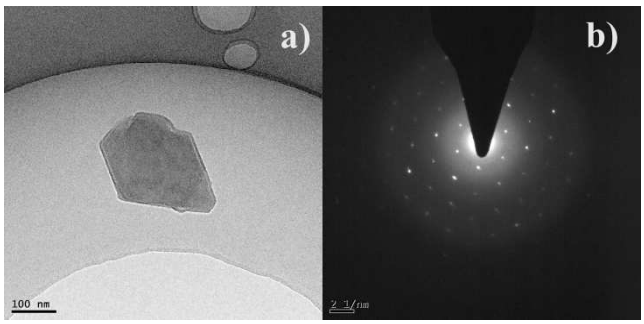

Fig. 6 TEM (a) and electron diffraction pattern (b) of the FJSM-SnS nanocrystal at pH ≈ 12.7.

As shown in Fig. S8, the PXRD patterns of ion-exchanged materials at a pH range from 0.7 to 11 were in good agreement with that of the pristine. When the pH was adjusted to 12.7, the FJSM-SnS bulk crystal was dissolved in the solution. But as shown in Fig. 6a and 6b, the bulk crystals were dispersed as nanocrystals into the solution and the crystal lattice was still kept well. The structural stability of FJSM-SnS is impressive over such wide pH range (from 0.7 to 12.7), which is very rare in the typical natural mineral ion-exchangers.

In the individual pH dependent ion-exchange experiments, the K_d (Cs^+) ranges from 898 mL/g (pH ≈ 0.7) to 2355 mL/g (pH ≈ 6.6) as shown in Fig. 7a. The K_d (Cs^+) at pH ≈ 1.4 is 1912 mL/g compared to 1180 mL/g of KMS-2 at pH ≈ 3. And the K_d (Sr^{2+}) could reach the value of 88863 mL/g in neutral solution, then decreased to 1708 mL/g (pH ≈ 3) and 2232 mL/g (pH ≈ 10). It demonstrates that FJSM-SnS is an effective Cs^+ and Sr^{2+} ion-exchanger over wide pH, even in extreme acid or alkali conditions. Compared to the other ion-exchangers,[11] the title compound exhibits super acid and alkali resistance.

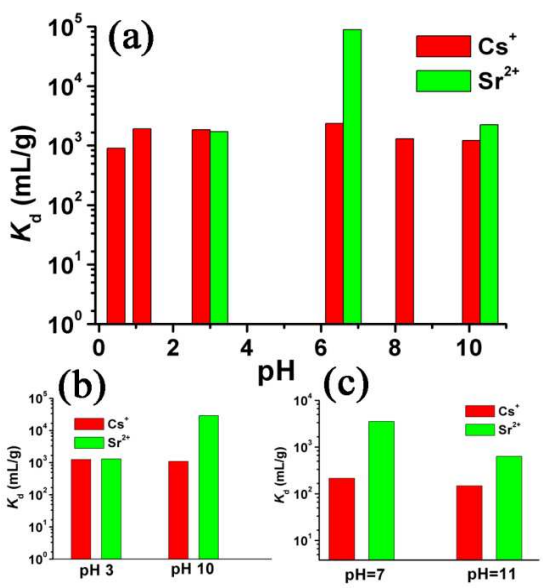

Fig. 7 (a) The K_d of Cs^+ and Sr^{2+} in individual pH dependent ion-exchange experiments (C_0 in the range of 5-8 ppm for Cs^+ and 2-7 ppm for Sr^{2+}, V:m = 1000 mL/g, at 65 °C); (b) the K_d of Cs^+ and Sr^{2+} in competitive ion-exchange experiments with the coexistence of Cs^+ and Sr^{2+} ions at extreme pH conditions (C_0 in the range of 5-7 ppm for both Cs^+ and Sr^{2+}, V:m = 1000 mL/g, at 65 °C); (c) the K_d of Cs^+ and Sr^{2+} in the simulated neutral and alkaline groundwater (C_0 ~ 2 ppm for Cs^+, C_0 ~ 6 ppm for Sr^{2+}, at 65 °C).

Besides the individual pH dependent experiments, the interaction between Cs^+ and Sr^{2+} ions at extreme pH has also been discussed. The competitive ion-exchange results (Fig. 7b) are almost as the same as the individual. But the K_d (Sr^{2+}) has increased from 2232 mL/g to 29051 mL/g when Cs^+ coexisted in the pH ≈ 10 solution. The synergistic effect between Cs^+ and Sr^{2+} could also be found in the KMS-2.[3]

3.5 Ion-exchange in the simulated groundwater

The ion-exchange performance in the simulated groundwater has been further explored. The solution containing a variety of cations such as Ca^{2+}, Mg^{2+}, K^+, Na^+ and Cs^+ or Sr^{2+} ions were used to simulate groundwater.[33] In the simulated groundwater, K_d (Cs^+) is 2.15 × 10^2 mL/g at pH ≈ 7 and 1.48 × 10^2 mL/g at pH ≈ 11, while K_d (Sr^{2+}) is 3.53 × 10^3 mL/g at pH ≈ 7 and 6.32 × 10^2 mL/g at pH ≈ 11, Fig. 7c. Because the constituents and their concentrations in the simulated groundwater are inconsistent in different reports,[3, 33, 34] it is hard to make a detailed comparison of K_d among different materials. The general affinity order of FJSM-SnS was Sr^{2+} > Ca^{2+} > Mg^{2+} > Cs^{2+} > K^+ (Table S2). In addition, two sets of competitive ion-exchange experiments using a molar 10:10:10:1 ratio of Na^+, K^+, Rb^+ and Cs^+ ions and a molar 10:10:10:1 ratio of Mg^{2+}, Ca^{2+}, Ba^{2+} and Sr^{2+} ions have been performed, respectively. The K_d values of Cs^+ or Sr^{2+} are still several times of those of lighter elements in the same group (Table S3 and S4). For example, the K_d value of Cs^+ is more than 5 times of that of K^+. The results were in accordance with the fact that the metal chalcogenides preferred the softer ions and higher charge state ions. The data in Table S2 also suggested that the higher removal rate could be achieved in the lower V:m ratio system, which should be attributed to the more available exchange sites.[33]

3.6 Ion-exchange chromatography

The performance of the ion-exchange chromatographic column filled with 3 g of the FJSM-SnS crystals has been demonstrated at room temperature. The detail could be found in the experimental section. The removal rates (R) of Cs^+ and Sr^{2+} were calculated by:

$$R = \frac{(C_0 - C_t)}{C_0} \times 100\% \qquad (4)$$

In equation 4, C_0 is the initial concentration and C_t is the concentration in the outlet solution when a certain volume solution was processed.

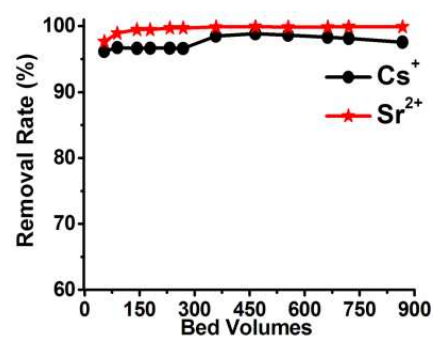

Fig. 8 The removal rates of Cs^+ and Sr^{2+} are plotted against bed volumes, respectively.

During the treatment of 900 bed volumes (total volume = 2.42 L, bed volume = 2.79 mL) mixing solutions of Cs^+ (C_0: 12 ~ 14.5 ppm) and Sr^{2+} (C_0: 5.98 ppm), there was no deterioration of the removal rate (Fig. 8). And the fluctuation accounted for the dynamic exchange process existed in the Cs^+ removal curve. The result indicated that ion-exchange chromatographic column filled with FJSM-SnS crystals could remove 96% ~ 99% Cs^+ and almost 100% Sr^{2+}, respectively.

As mentioned above, the maximum Cs^+ exchange capacity of FJSM-SnS is 1.8 times that of KMS-1 and far more than those of commercial AMP-PAN and TAM-5. Such a big ion exchange capacity for Cs^+ ion can be attributed to the stronger affinity of soft Lewis basic S^{2-} ions for softer Lewis acidic Cs^+ ion than harder $[Me_2NH_2]^+$ and $[Me_3NH]^+$ cations, as well as its two-dimensionally microporous and flexible open-framework enabling the guest cations to diffuse in and out of the material.[32, 43, 44, 74] Both the $[Me_2NH_2]^+$ and $[Me_3NH]^+$ cations located at the interlayer spaces are able to be exchanged. The material still remains good crystalline structure after ion-exchange which can also be ascribed to the stability and flexibility of framework. Furthermore, it could reach rapid ion-exchange equilibrium within 5 minutes, which is much faster than other kinds of ion-exchangers. The pH resistance (0.7 ~ 12.7) of FJSM-SnS is much wider than those of most of the ion-exchangers. The ion-exchange column mode operation, which hasn't been studied in chalcogenido ion-exchange materials before, has also been further conducted with good performance.

4. Conclusions

In conclusion, a robust, uniform, high cost-efficient layered thiostannate as ion-exchange material could be synthesized in large-scale by a facile, one-pot and economically solvothermal method, which revealed the abilities of fast ion capture, strong ion-exchange capacity and super acid and alkali resistance. The kinetic and isothermal studies of Cs^+ and Sr^{2+} ion-exchange, pH dependent experiments, simulated environments and ion-exchange chromatography have been studied in depth. In particular, the ion-exchange chromatographic column is firstly performed in chalcogenido ion-exchange materials, which promotes a big step towards the practical application of chalcogenido ion-exchanger. The title compound with the relatively low-cost but remarkable ion-exchange performance represents a new potential material of radioactive Cs^+ and Sr^{2+} remediation. It is expected that more $A_2Sn_3S_7$ materials templated by small organic amines can be developed to deal with radioactive and heavy metal ions.

Acknowledgements

Xing-Hui Qi and Dr. Ke-Zhao Du contributed equally to this work. Financial supports from the NNSF of China (Nos. 21373223 and 21221001) and Chunmiao project of Haixi institute of Chinese Academy of Sciences (CMZX-2014-001) are greatly acknowledged.

Notes and references

[a] *State Key Laboratory of Structural Chemistry, Fujian Institute of Research on the Structure of Matter, Chinese Academy of Sciences, Fuzhou, Fujian 350002, P. R. China; E-mail: fml@fjirsm.ac.cn*
[b] *College of Chemistry, Fuzhou University, Fuzhou, Fujian 350002, P. R. China.*
[c] *University of Chinese Academy of Sciences, Beijing 100049, P. R. China*

† Electronic Supplementary Information (ESI) available: Crystallographic data for FJSM-SnS and FJSM-SnS-Cs in CIF format, TG-MS spectra, mass spectra of solution and solvent, PXRD, EDS, the kinetics studies at room temperature, IR and table of data in the simulated groundwater, competitive ion-exchange experiments and the ion-exchange chromatographic column experiment. CCDC 1025383 for FJSM-SnS and CCDC 1025384 for Cs^+-exchanged FJSM-SnS. See DOI: 10.1039/b000000x/.

1. Z. Yang, M. Kang, B. Ma, J. Xie, F. Chen, L. Charlet and C. Liu, *Environ. Sci. Technol.*, 2014, **48**, 10716-10724.
2. T. Vincent, C. Vincent, Y. Barre, Y. Guari, G. Le Saout and E. Guibal, *J. Mater. Chem. A*, 2014, **2**, 10007-10021.
3. J. L. Mertz, Z. H. Fard, C. D. Malliakas, M. J. Manos and M. G. Kanatzidis, *Chem. Mater.*, 2013, **25**, 2116-2127.
4. L. Al-Attar, A. Dyer, A. Paajanen and R. Harjula, *J. Mater. Chem.*, 2003, **13**, 2969-2974.
5. P. Sylvester, T. Milner and J. Jensen, *J. Chem. Technol. Biotechnol.*, 2013, **88**, 1592-1596.
6. J. M. Arnal, M. Sancho and B. Garcia-Fayos, *Desalination*, 2013, **321**, 22-27.
7. N. L. Torad, M. Hu, M. Imura, M. Naito and Y. Yamauchi, *J. Mater. Chem.*, 2012, **22**, 18261-18267.
8. N. Yoshida and J. Kanda, *Science*, 2012, **336**, 1115-1116.
9. http://www.world-nuclear.org/info/Nuclear-Fuel-Cycle/Nuclear-Wastes/Waste-Management-Overview/, vol. 2012.
10. A. Verbruggen, *Energ. Policy*, 2008, **36**, 4036-4047.
11. R. O. A. Rahman, H. A. Ibrahium and Y. T. Hung, *Water*, 2011, **3**, 551-565.
12. D. V. Marinin and G. N. Brown, *Waste Manage.*, 2000, **20**, 545-553.
13. J. Lehto and R. Harjula, *Radiochim. Acta*, 1999, **86**, 65-70.
14. K. M. L. Taylor-Pashow, T. C. Shehee and D. T. Hobbs, *Solvent Extr. Ion Exch.*, 2013, **31**, 122-170.
15. A. Clearfield, *Solvent Extr. Ion Exch.*, 2000, **18**, 655-678.
16. S. Komarneni and R. Roy, *Nature*, 1982, **299**, 707-708.
17. Y. Lan, Z. Su, X. L. Li, Z. Q. Jiang, J. Jin, J. L. Xie and S. J. Li, *J. Radioanal. Nucl. Chem.*, 2007, **273**, 99-102.
18. H. Luhrs, J. Derr and R. X. Fischer, *Micropor. Mesopor. Mat.*, 2012, **151**, 457-465.
19. A. Dyer, A. Chimedtsogzol, L. Campbell and C. Williams, *Micropor. Mesopor. Mat.*, 2006, **95**, 172-175.
20. A. Abusafa and H. Yucel, *Sep. Purif. Technol.*, 2002, **28**, 103-116.
21. A. Tripathi, J. B. Parise, S. J. Kim, Y. Lee, G. M. Johnson and Y. S. Uh, *Chem. Mater.*, 2000, **12**, 3760-3769.
22. B. H. Fawaris and K. J. Johanson, *Sci. Total Environ.*, 1995, **172**, 251-256.
23. T. P. Valsala, S. C. Roy, J. G. Shah, J. Gabriel, K. Raj and V. Venugopal, *J. Hazard. Mater.*, 2009, **166**, 1148-1153.
24. M. M. Ishfaq, H. M. A. Karim and M. A. Khan, *J. Radioanal. Nucl. Chem.*, 1993, **170**, 321-331.
25. I. M. Ali, E. S. Zakaria and H. F. Aly, *J. Radioanal. Nucl. Chem.*, 2010, **285**, 483-489.

26. A. J. Celestian, J. D. Kubicki, J. Hanson, A. Clearfield and J. B. Parise, *J. Am. Chem. Soc.*, 2008, **130**, 11689-11694.
27. A. J. Celestian and A. Clearfield, *J. Mater. Chem.*, 2007, **17**, 4839-4842.
28. A. Clearfield, S. Solbrå, N. Allison, S. Waite, S. V. Mikhalovsky, A. I. Bortun and L. N. Bortun, *Environ. Sci. Technol.*, 2001, **35**, 626-629.
29. B. J. Riley, J. Chun, W. Um, W. C. Lepry, J. Matyas, M. J. Olszta, X. Li, K. Polychronopoulou and M. G. Kanatzidis, *Environ. Sci. Technol.*, 2013, **47**, 7540-7547.
30. M. J. Manos and M. G. Kanatzidis, *J. Am. Chem. Soc.*, 2012, **134**, 16441-16446.
31. A. Clearfield, *Nat. Chem.*, 2010, **2**, 161-162.
32. N. Ding and M. G. Kanatzidis, *Nat. Chem.*, 2010, **2**, 187-191.
33. M. J. Manos and M. G. Kanatzidis, *J. Am. Chem. Soc.*, 2009, **131**, 6599-6607.
34. M. J. Manos, N. Ding and M. G. Kanatzidis, *Proc. Natl. Acad. Sci. U. S. A.*, 2008, **105**, 3696-3699.
35. M. J. Manos, K. Chrissafis and M. G. Kanatzidis, *J. Am. Chem. Soc.*, 2006, **128**, 8875-8883.
36. M. J. Manos, R. G. Iyer, E. Quarez, J. H. Liao and M. G. Kanatzidis, *Angew. Chem., Int. Ed.*, 2005, **44**, 3552-3555.
37. M. J. Manos, C. D. Malliakas and M. G. Kanatzidis, *Chem.- Eur. J.*, 2007, **13**, 51-58.
38. N. Ding and M. G. Kanatzidis, *Chem. Mater.*, 2007, **19**, 3867-3869.
39. K. Chondroudis and M. G. Kanatzidis, *J. Solid State Chem.*, 1998, **136**, 328-332.
40. T. J. McCarthy, T. A. Tanzer and M. G. Kanatzidis, *J. Am. Chem. Soc.*, 1995, **117**, 1294-1301.
41. N. Ding and M. G. Kanatzidis, *Angew. Chem., Int. Ed.*, 2006, **45**, 1397-1401.
42. P. Sengupta, N. L. Dudwadkar, B. Vishwanadh, V. Pulhani, R. Rao, S. C. Tripathi and G. K. Dey, *J. Hazard. Mater.*, 2014, **266**, 94-101.
43. M. L. Feng, D. N. Kong, Z. L. Xie and X. Y. Huang, *Angew. Chem., Int. Ed.*, 2008, **47**, 8623-8626.
44. J. R. Li and X. Y. Huang, *Dalton Trans.*, 2011, **40**, 4387-4390.
45. M. J. Manos and M. G. Kanatzidis, *Chem.- Eur. J.*, 2009, **15**, 4779-4784.
46. S. Dafauti, V. Pulhani and A. G. Hegde, *Desalin. Water Treat.*, 2012, **38**, 264-270.
47. M. J. Manos, V. G. Petkov and M. G. Kanatzidis, *Adv. Funct. Mater.*, 2009, **19**, 1087-1092.
48. S. J. Datta, W. K. Moon, D. Y. Choi, I. C. Hwang and K. B. Yoon, *Angew. Chem., Int. Ed.*, 2014, **53**, 1-7.
49. N. Staelens, M. F. Reyniers and G. B. Marin, *Ind. Eng. Chem. Res.*, 2004, **43**, 5123-5132.
50. G. A. Marking and M. G. Kanatzidis, *Chem. Mater.*, 1995, **7**, 1915-1921.
51. K. M. Tan, Y. G. Ko and J. B. Parise, *Acta Crystallogr. C*, 1995, **51**, 398-401.
52. T. Jiang, A. Lough and G. A. Ozin, *Adv. Mater.*, 1998, **10**, 42-43.
53. T. Jiang, A. Lough, G. A. Ozin and R. L. Bedard, *J. Mater. Chem.*, 1998, **8**, 733-741.
54. T. Jiang, A. Lough, G. A. Ozin, R. L. Bedard and R. Broach, *J. Mater. Chem.*, 1998, **8**, 721-732.
55. C. L. Bowes, S. Petrov, G. Vovk, D. Young, G. A. Ozin and R. L. Bedard, *J. Mater. Chem.*, 1998, **8**, 711-720.
56. T. Jiang and G. A. Ozin, *J. Mater. Chem.*, 1998, **8**, 1099-1108.
57. T. Jiang, G. A. Ozin, A. Verma and R. L. Bedard, *J. Mater. Chem.*, 1998, **8**, 1649-1656.
58. H. Ahari, C. L. Bowes, T. Jiang, A. Lough, G. A. Ozin, F. L. Bedard, S. Petrov and D. Young, *Adv. Mater.*, 1995, **7**, 375-378.
59. J. B. Parise, Y. H. Ko, J. Rijssenbeek, D. M. Nellis, K. M. Tan and S. Koch, *Chem. Commun.*, 1994, 527-527.
60. W. S. Sheldrick and B. Schaaf, *Z. Anorg. Allg. Chem.*, 1994, **620**, 1041-1045.
61. A. M. El-Kamash, *J. Hazard. Mater.*, 2008, **151**, 432-445.
62. X. L. Li, B. J. Liu, Y. Jian, W. B. Zhong, W. J. Mu, J. H. He, Z. P. Ma, G. P. Liu and S. Z. Luo, *Sep. Sci. Technol.*, 2012, **47**, 896-902.
63. C. C. Pavel, K. Popa, N. Bilba, A. Cecal, D. Cozma and A. Pui, *J. Radioanal. Nucl. Chem.*, 2003, **258**, 243-248.
64. C. C. Pavel and K. Popa, *Chem. Eng. J.*, 2014, **245**, 288-294.
65. C. C. Pavel, D. Vuono, A. Nastro, J. B. Nagy and N. Bilba, *Stud. Surf. Sci. Catal.*, 2002, **142**, 295-302.
66. N. Dobelin and T. Armbruster, *Micropor. Mesopor. Mat.*, 2007, **99**, 279-287.
67. M. E. Huckman, I. M. Latheef and R. G. Anthony, *Sep. Sci. Technol.*, 1999, **34**, 1145-1166.
68. K. Popa and C. C. Pavel, *Desalination*, 2012, **293**, 78-86.
69. C. C. Pavel, M. Walter, P. Poml, D. Bouexiere and K. Popa, *J. Mater. Chem.*, 2011, **21**, 3831-3837.
70. Y. Park, Y. C. Lee, W. S. Shin and S. J. Choi, *Chem. Eng. J.*, 2010, **162**, 685-695.
71. T. J. Tranter, R. S. Herbst, T. A. Todd, A. L. Olson and H. B. Eldredge, *Adv. Environ. Res.*, 2002, **6**, 107-121.
72. Z. Zheng, C. V. Philip, R. G. Anthony, J. L. Krumhansl, D. E. Trudell and J. E. Miller, *Ind. Eng. Chem. Res.*, 1996, **35**, 4246-4256.
73. R. P. Han, W. H. Zou, Y. Wang and L. Zhu, *J. Environ. Radioact.*, 2007, **93**, 127-143.
74. M. L. Feng, X. H. Qi, B. Zhang and X. Y. Huang, *Dalton Trans.*, 2014, **43**, 8184-8187.

TOC

A two-dimensionally microporous thiostannate with superior Cs^+ and Sr^{2+} ion-exchange property

Xing-Hui Qi, Ke-Zhao Du, Mei-Ling Feng*, Jian-Rong Li, Cheng-Feng Du, Bo Zhang and Xiao-Ying Huang

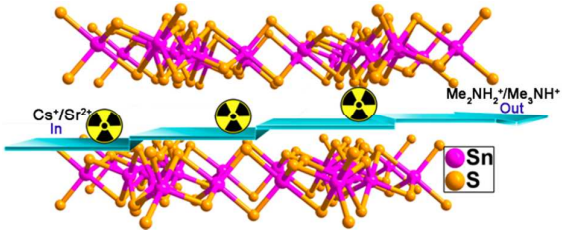

A layered thiostannate with the remarkable Cs^+ and Sr^{2+} ion-exchange performance was synthesized in large-scale by a facile, one-pot, economically solvothermal methods.